Original Article

Plasma proteomic profiling reveals biomarkers associated with aortic dilation in patients with bicuspid aortic valve

Wenrui Ma[1], Jingjing Zhang[2], Kehua Xu[2], Shiqiang Yan[2], Dingqian Liu[1], Hui Huang[2], Yuyi Tang[2], Guoquan Yan[2], Yongxin Sun[1], Jun Li[1], Weijia Zhang[2], Chunsheng Wang[1], Kai Zhu[1], Hao Lai[1]

[1]Department of Cardiac Surgery and Shanghai Institute of Cardiovascular Diseases, Zhongshan Hospital, Fudan University, Shanghai, China; [2]Institutes of Biomedical Sciences and Shanghai Key Laboratory of Medical Imaging Computing and Computer-Assisted Intervention, Shanghai Medical College, Fudan University, Shanghai, China

Contributions: (I) Conception and design: W Zhang, K Zhu, C Wang, H Lai; (II) Administrative support: W Zhang, K Zhu, C Wang, H Lai; (III) Provision of study materials or patients: Y Sun, J Li, K Zhu, C Wang, H Lai; (IV) Collection and assembly of data: W Ma, J Zhang, K Xu, S Yan, D Liu, H Huang, Y Tang, G Yan, Y Sun, J Li; (V) Data analysis and interpretation: W Ma, J Zhang, K Xu, S Yan; (VI) Manuscript writing: All authors; (VII) Final approval of manuscript: All authors.

Correspondence to: Kai Zhu, MD, PhD; Chunsheng Wang, MD; Hao Lai, MD. Department of Cardiac Surgery and Shanghai Institute of Cardiovascular Diseases, Zhongshan Hospital, Fudan University, 180 Fenglin Road, Shanghai 200032, China. Email: zhu.kai1@zs-hospital.sh.cn; wangchunsheng@fudan.edu.cn; lai.hao@zs-hospital.sh.cn.

Background: Bicuspid aortic valve (BAV) is the most common congenital heart anomaly and is prone to cause complications, such as valvular stenosis and thoracic aortic dilation. There is currently no reliable way to predict the progression rate to thoracic aortic aneurysm. Here, we aimed to characterize the proteomic landscape in the plasma of stenotic BAV patients and provide potential biomarkers to predict progressive aortic dilation.

Methods: Plasma samples were obtained from 45 subjects (30 stenotic BAV patients and 15 healthy controls). All samples were properly prepared and analyzed using mass spectrometry (MS)-based label-free quantitative proteomics.

Results: A total of 748 plasma proteins had missingness <50%, and 193 (25.8%) were differentially expressed in the BAV patients. Functions regarding cell junction and actin cytoskeleton were largely enriched. *NOTCH3*, a Notch receptor known to interact with the BAV-causing gene *NOTCH1*, was negatively correlated with aortic diameter and was downregulated in BAV patients' plasma and aortic smooth muscle cells. Further, a subset of plasma proteins, including *ADAM10*, was associated with rapidly progressive aortic dilation in BAV patients.

Conclusions: Our data reveal unique features in the proteomic architecture of stenotic BAV patients' plasma, and we propose the potential of Notch signaling proteins *NOTCH3* and *ADAM10* in predicting aortic dilation.

Keywords: Plasma proteomics; bicuspid aortic valve (BAV); aortic dilation; biomarker; Notch signaling

Submitted May 18, 2021. Accepted for publication Jul 13, 2021.
doi: 10.21037/atm-21-3378
View this article at: https://dx.doi.org/10.21037/atm-21-3378

Introduction

Bicuspid aortic valve (BAV) is the most frequent congenital heart anomaly affecting approximately 1.4% of the general population (1-3). Ascending aortic disease is a common complication of a stenotic BAV, characterized by progressive aortic dilation (i.e., an increase in the aortic diameter) that may lead to aneurysm formation and lethal events such as aortic dissection and rupture (4-6). Currently, there is no

validated method to predict the progression rate of aortic dilation in BAV patients, thus posing an obstacle to clinical decision-making regarding the optimal timing for aortic surgery (7,8). Plasma proteins have emerged as a useful source of biomarkers to reflect aortic pathology at the tissue level (9,10) but have not been comprehensively profiled in BAV patients with aortic dilation.

In this study, we collected plasma samples from stenotic BAV patients and healthy controls. By mass spectrometry (MS)-based proteomic analysis, the entire list of the differentially expressed proteins (DEPs) was identified and characterized. Further, the ascending aortic diameters of the BAV patients were measured during follow-up, and the DEPs were screened for potential biomarkers that were closely related to progressive aortic dilation. We present the following article in accordance with the MDAR reporting checklist (available at https://dx.doi.org/10.21037/atm-21-3378).

Methods

Study subjects and materials

In this study, we included adult patients with stenotic BAV who were hospitalized at our institution between December 2017 and November 2018. Exclusion criteria included patients with connective tissue disorder, predominant aortic valve regurgitation, or a history of cardiac surgery. After screening, a total of 30 eligible candidates were enrolled, including 17 patients with significant aortic dilation (ascending aortic diameter >45 mm) and 13 without (diameter ≤45 mm). We further recruited 15 healthy volunteers without cardiovascular diseases (ascending aortic diameter ≤35 mm) as the control group. To evaluate the plasma proteins' capacity to reflect pathologies in the aortic cells, we harvested and expanded primary aortic smooth muscle cells from an additional three BAV patients with significant aortic dilation and from two controls with non-diseased ascending aortas, using the aortic explant technique (11). For all cell experiments, the passage number was limited to six. This study was approved by Zhongshan Hospital Fudan University Ethics Committee (Approval Letter No. B2020-158R), and written consent was obtained from all study subjects. All procedures performed in this study involving human participants were in accordance with the Declaration of Helsinki (as revised in 2013).

Sample preparation for MS analysis

Plasma samples were collected from all patients and volunteers and depleted using the High Select™ Top14 Abundant Protein Depletion mini column (Thermo Fisher Scientific). After measuring the plasma protein concentration (Pierce BCA, Thermo Fisher Scientific), 50 μg protein for each sample were reduced with 10 mM dithiothreitol (final concentration) for 30 minutes at 37 ℃ and alkylated with 55 mM iodoacetamide (final concentration) for an additional 30 minutes at room temperature. The remaining detergent was removed by acetone precipitation, and protein pellets were resolved in 50 μL 6 M urea (in 10 mM Hepes, pH 8.0) and digested with 0.5 μg LysC for 3 hours at room temperature. After adding four volumes of 50 mM ammonium bicarbonate, tryptic digestion was carried out overnight. On the next day, digestion was stopped by adding 1% trifluoroacetic acid. Peptides were finally desalted on C18 Stage Tips and kept at –80 ℃ until MS analysis.

Liquid chromatography-MS analysis

MS analysis was performed using a Quadrupole Orbitrap mass spectrometer (Q Exactive HF, Thermo Fisher Scientific) coupled to a Waters uHPLC system via a nano-electrospray source. Columns were packed with 1.9 mm C18 particles (Thermo Fisher Scientific). Peptides were separated over a 250-minute gradient from 2% to 60% in buffer B (80% acetonitrile, 0.5% formic acid) at 200 nL/minute. The column temperature was constantly set to 50 ℃ using a column oven. The survey scans were acquired with a resolution of 60,000 for Q Exactive HF, at m/z 200. A top 15 method was used to select the most abundant precursor ions with a charge Z^{2+}. Selected precursor ions were subjected to high-energy collisional dissociation fragmentation at a normalized collision energy of 27, an isolation window of 1.4 Th, and a resolution of 15,000 at m/z 200. For survey scans, ion injection times were set to 20 milliseconds (target value 3E6) and 120 milliseconds (target value 1E5) for MS/MS scans. Dynamic exclusion of sequenced peptides was set to 30 seconds. Data were acquired using Xcalibur software (Thermo Fisher Scientific).

MS data analysis

MS raw files were analyzed using MaxQuant software (Computational Systems Biochemistry). Proteins with missing values <50% were filled using k Nearest Neighbors followed by normalization using the edgeR R package

(version 3.28.1) (12,13). The limma R package (version 3.42.2) was used to examine whether proteins were differentially expressed between BAV and control groups and between BAV patients with and without progressive aortic dilation (14). Proteins with P values <0.05, and fold-change ratios >1.5 were considered significant. Annotation and functional enrichment were performed using the Metascape database (http://metascape.org) and the Ingenuity Pathway Analysis (IPA, QIAGEN), and protein-protein interactions were searched using the STRING database (15-18). The comparative proteomics datasets are uploaded online (https://cdn.amegroups.cn/static/public/atm-21-3378-1.xlsx). The raw MS data files are available from the corresponding authors upon reasonable request.

Criterion for progressive aortic dilation

In this study, 17 stenotic BAV patients with an ascending aortic diameter ≥45 mm underwent aortic valve replacement and concomitant aortic repair, and 12 out of 13 patients with an ascending aortic diameter <45 mm underwent isolated valve replacement. Among these patients, nine were followed up at our institution after surgery. Given the potential interobserver variability in measuring aortic diameter, progressive aortic dilation was defined conservatively, i.e., a gradual increase in the ascending aortic diameter over time that reached ≥4 mm at the latest follow-up.

Quantitative real-time polymerase chain reaction (qRT-PCR)

The total RNA of the primary aortic smooth muscle cells expanded from BAV patients and controls were extracted using TRIzol agent (T9424, Sigma-Aldrich). Synthesis of complementary DNA and qRT-PCR was performed according to the manufacturer's guidelines (RR037B and RR420B, Takara). The expression levels of the following genes were investigated: *ADAM10* (forward: ATGGGAGGTCAGTATGGGAATC; reverse: ACTGCTCTTTTGGCACGCT), *HEY2* (forward: AAGGCGTCGGGATCGGATAA; reverse: AGAGCGTGTGCGTCAAAGTAG), *NOTCH3* (forward: TGGCGACCTCACTTACGACT; reverse: CACTGGCAGTTATAGGTGTTGAC), *SERPINE1* (forward: ACCGCAACGTGGTTTTCTCA; reverse: TTGAATCCCATAGCTGCTTGAAT), *SUMO4* (forward: CCACGGGGATTGTCAGTGAAG; reverse: CTGTGCAGGTTTGTCTGTTCC), *SVEP1* (forward: CAGCAGTTGCATTCCATGTCC; reverse: AAGTAACCATTTTCGGGAGGC), and *GAPDH* (forward: CTGGGCTACACTGAGCACC; reverse: AAGTGGTCGTTGAGGGCAATG).

Immunofluorescence

Immunofluorescence was performed on the diseased and control aortic smooth muscle cells. Briefly, cells were fixed in 4% paraformaldehyde at room temperature for 20 minutes and permeabilized with 0.1% Triton-X (X100, Sigma-Aldrich) solution at room temperature for 30 minutes. NOTCH3 and smooth muscle cell marker ACTA2 were stained using their respective primary antibodies (D11B8, Cell Signaling Technology; ab7817, Abcam) overnight at 4 ℃. After three washes with PBS, the samples were incubated with secondary antibodies (4412S and 8890S, Cell Signaling Technology) for 1 hour at 37 ℃. Nuclei were stained with 4',6-diamidino-2-phenylindole (DAPI, D1306, Invitrogen) for 5 minutes at room temperature. Representative images of three different regions of each sample were acquired using a fluorescence microscope (DMi8, Leica) and analyzed using ImageJ software (ver. 1.52n, National Institutes of Health).

Enzyme-linked immunosorbent assay (ELISA)

The concentration of ADAM10 in the supernatant of the BAV and control aortic smooth muscle cells was measured using a sandwich ELISA kit (JL13337, Jianglai Biology, Shanghai, China) that contained adhered anti-human ADAM10 antibodies. Secondary antibodies were used to bind to the adhered proteins and, after adding substrate to the enzyme, the absorbance reading of the plates was performed on a plate reader at 450 nm wavelength (AMR-100, Allsheng, Hangzhou, China).

Statistical analysis

Continuous variables were presented as means ± standard deviations or median (interquartile range), according to the normality test. Parameters were compared using the two-tailed *t*-test (normal distribution) or the Mann-Whitney U-test (skewed distribution). Categorical variables were expressed as numbers (percentages) and compared using Fisher's exact test or the Cochran-Mantel-Haenszel test, as appropriate. Correlation analysis was performed

using Pearson's correlation test. Analyses were performed using Prism v8.0 (GraphPad Software, Inc.). Statistical significance was indicated by two-tailed *P<0.05, *P<0.01, and ***P<0.001.

Results

Characteristics of the study population and the overall proteome

The study workflow is shown in *Figure 1A*, and the baseline demographics of the study subjects are listed in Table S1 and Table S2. There was no significant difference in age, gender, or other clinical parameters between the BAV patients and healthy controls. Using the plasma samples harvested from all candidates, proteomic analysis identified a total of 998 proteins, 748 of which had missingness <50%. Annotation showed the top 20 functions of these plasma proteins, including aortic disease-related functions such as insulin-like growth factor transport, extracellular matrix organization, and cell-substrate adhesion (*Figure 1B*). The principal component analysis suggested distinct proteomic profiles between BAV patients and healthy controls with marginal overlaying regions, while stratification by gender or age did not clearly distinguish the overall plasma proteome, suggesting the presence of independent features in the plasma of stenotic BAV patients (*Figure 1C*).

Analysis of DEPs between BAV patients and controls

The comparative analysis yielded a total of 193 DEPs (*Figure 2A*; Table S3). Disease enrichment analysis revealed cardiovascular diseases such as vascular disease and abdominal aortic aneurysm (Figure S1). The integrated process enrichment analysis using Metascape showed a network of enriched terms, including regulated exocytosis, platelet degranulation, extracellular structure organization, and others (Figure S2). The canonical pathway enrichment analysis using IPA software indicated that the DEPs were related to epithelial adherens junction, RhoA signaling, integrin signaling, and actin cytoskeleton signaling (*Figure 2B*). The top upstream regulators included ADAM metallopeptidase domain 10 (*ADAM10*), matrix metallopeptidase 12 (*MMP12*), transforming growth factor beta 1 (*TGFB1*), and GATA binding protein 4 (*GATA4*), all of which are associated with thoracic aortic aneurysm (*Figure 2C*) (19-21). Notably, *ADAM10* is a regulator of the Notch signaling pathway that causes BAV formation (22-24). Since components and concentrations of plasma proteins could be influenced by alterations in the whole human body, 16 DEPs that are involved in several aortic diseases were screened (*Figure 2D*), including collagen type I alpha 1 chain (*COL1A1*), fibrillin-1 (*FBN1*), filamin A (*FLNA*), and notch receptor 3 (*NOTCH3*), which were closely interacted in a protein network (*Figure 2E*) (5,25). Expression-trait correlation analysis showed that *NOTCH3* was independently associated with the ascending aortic diameter. Expressions of *COL1A1* and *FBN1* were poorly correlated with aortic size, and *FLNA* expression was significantly influenced by the patient's age (*Figure 2F*).

NOTCH3 was consistently downregulated in the plasma and aortic cells of BAV patients

The Notch receptors have an overlapping effect on the development of multiple cardiovascular diseases (26). Mutation of the *NOTCH1* gene is a known causative factor of BAV and thoracic aortic aneurysm (24), whereas the role of *NOTCH3* in such diseases remains unclear. The correlation between the plasma level of *NOTCH3* and the ascending aortic diameter was in a negative direction (*Figure 3A*). Analysis of the protein-protein interactions indicated a close relationship across *NOTCH1*, *NOTCH3*, and *ADAM10* (*Figure 3B*). Further, qRT-PCR showed downregulation of *NOTCH3* and its downstream effector [hes related family bHLH transcription factor with YRPW motif 2 (*HEY2*)] in the aortic smooth muscle cells of BAV patients (*Figure 3C*). The immunofluorescence analysis also showed reduced levels of *NOTCH3* and *ACTA2* in diseased cells (*Figure 3D*).

DEPs between patients with and without progressive aortic dilation

The follow-up measurement of ascending aortic diameters is shown in *Figure 4A*. Progressive aortic dilation that reached the surgical threshold was present in two patients (4). The baseline characteristics of patients with and without progressive aortic dilation were comparable. Comparative proteomic analysis identified a total of 74 DEPs (*Figure 4B*; Table S4). When compared with the DEPs between BAV patients and controls, 23 proteins were overlapped. Notably, we identified 11 proteins exhibiting consistent changing trends in both comparisons (*Figure 4C*). Top-hit proteins such as *ADAM10*, plasminogen activator inhibitor 1 (*SERPINE1*), small ubiquitin-like

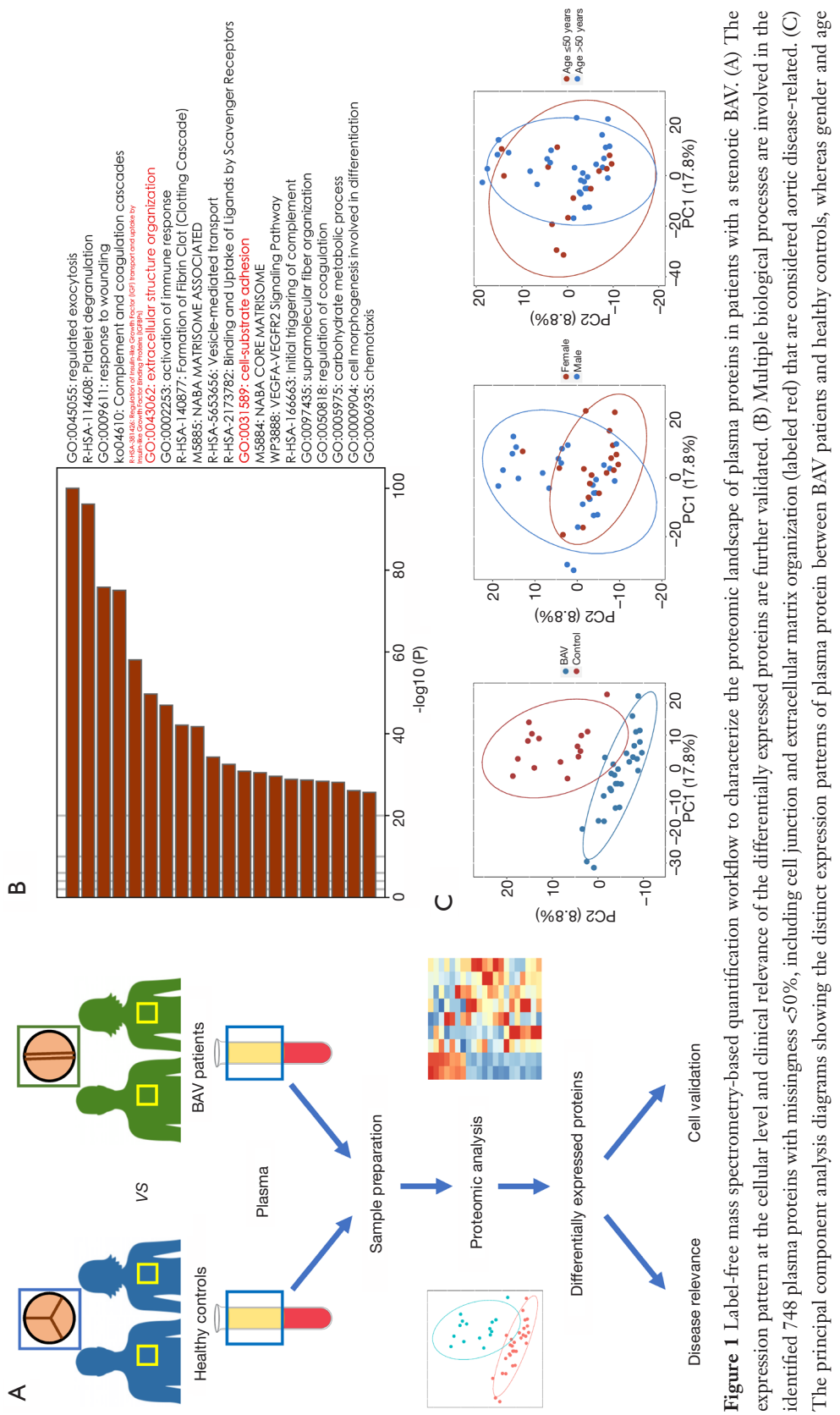

Figure 1 Label-free mass spectrometry-based quantification workflow to characterize the proteomic landscape of plasma proteins in patients with a stenotic BAV. (A) The expression pattern at the cellular level and clinical relevance of the differentially expressed proteins are further validated. (B) Multiple biological processes are involved in the identified 748 plasma proteins with missingness <50%, including cell junction and extracellular matrix organization (labeled red) that are considered aortic disease-related. (C) The principal component analysis diagrams showing the distinct expression patterns of plasma protein between BAV patients and healthy controls, whereas gender and age did not significantly influence the overall proteome. BAV, bicuspid aortic valve.

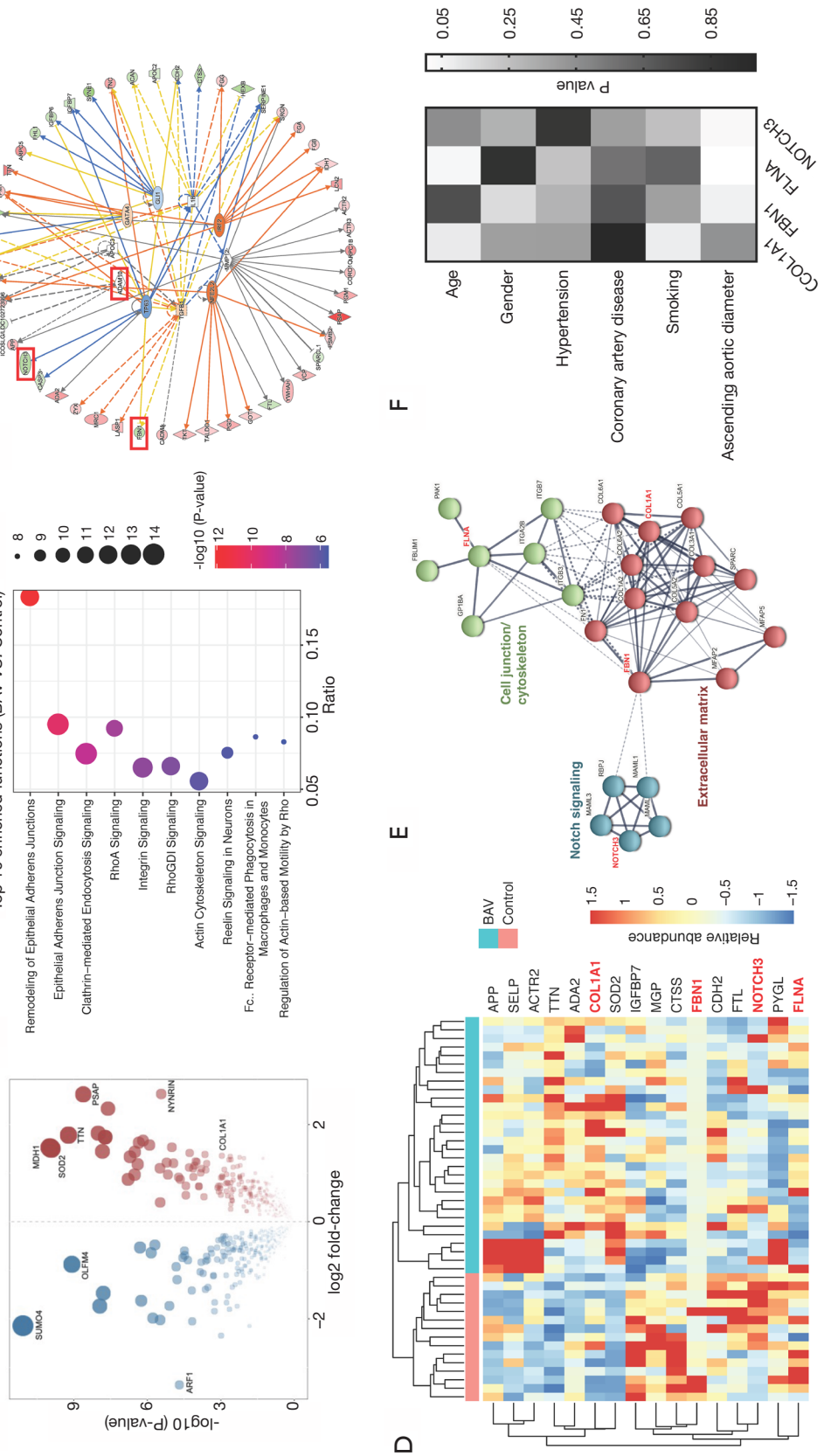

Figure 2 Comparative proteomic analysis of plasma proteins in stenotic BAV patients and controls. (A) The volcano map illustrating the DEPs. (B) The top 10 functions enriched by IPA software show cell junction and cytoskeleton signaling are largely involved in BAV patients. (C) Analysis of upstream regulators revealing several proteins that might regulate the expression of the DEPs. (D,E) From the 192 DEPs, 16 proteins associated with cardiovascular diseases are screened. Four proteins [*COL1A1*, *FBN1*, *NOTCH3*, and *FLNA* (labeled red)] known to be aortic aneurysm-related have close protein-protein interactions. (F) Correlations between concentrations of the 4 plasma proteins and clinical traits. BAV, bicuspid aortic valve; DEPs, differentially expressed proteins.

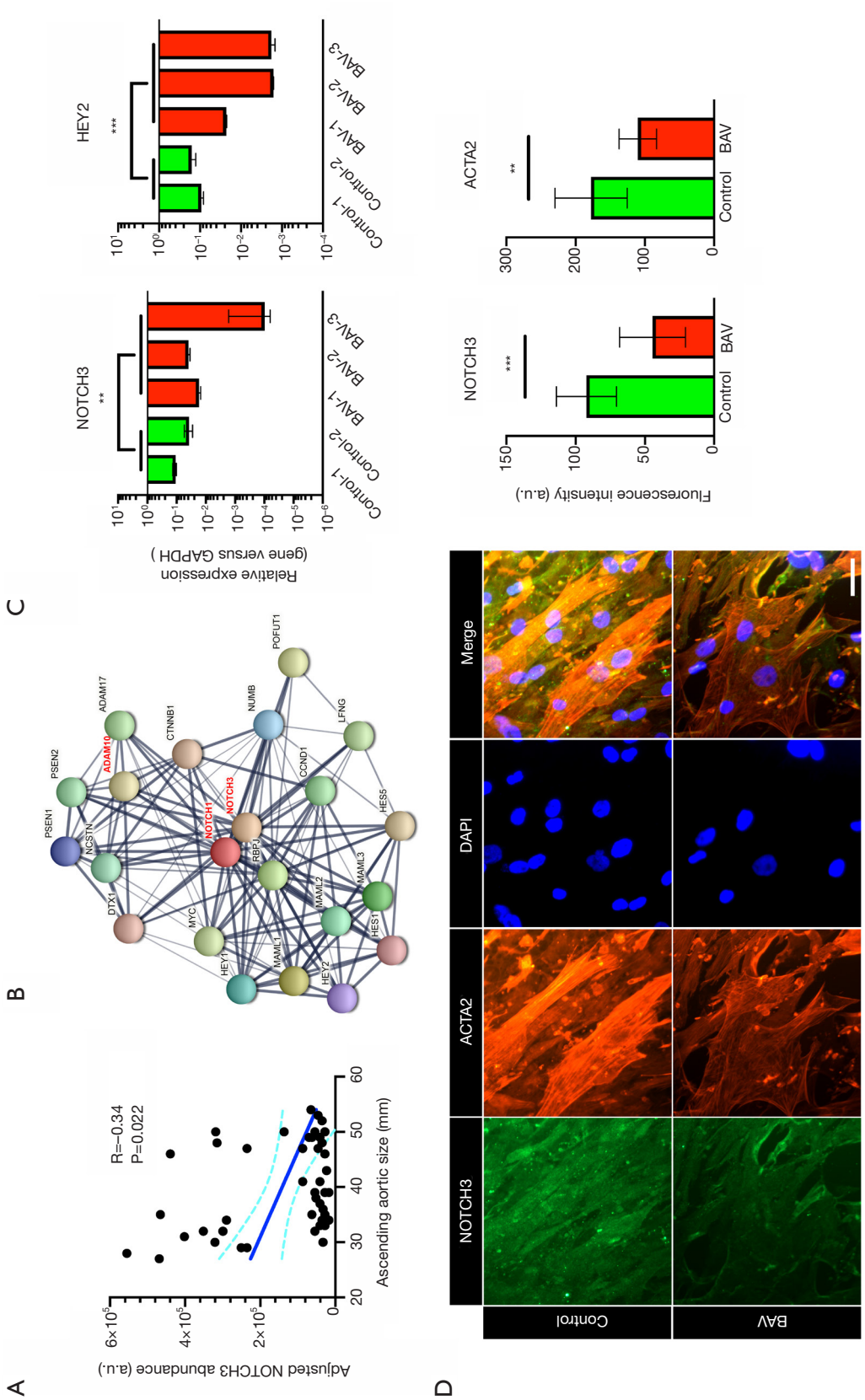

Figure 3 Expression of *NOTCH3* in stenotic BAV patients. (A) Pearson's correlation test revealing the negative correlation between the *NOTCH3* plasma level and the ascending aortic diameter. (B) Protein-protein interactions are present across *NOTCH1*, *NOTCH3*, *ADAM10*, and others. (C) qRT-PCR results showing downregulation of *NOTCH1* and *NOTCH3* in the aortic smooth muscle cells of stenotic BAV patients (n=3). (D) Immunofluorescence analysis demonstrating lowered *NOTCH3* and *ACTA2* expressions in the aortic smooth muscle cells of stenotic BAV patients (n=9). Scale bar: 50 μm. Values are presented as median and interquartile range. **P<0.01, and ***P<0.001. BAV, bicuspid aortic valve; qRT-PCR, quantitative real-time polymerase chain reaction.

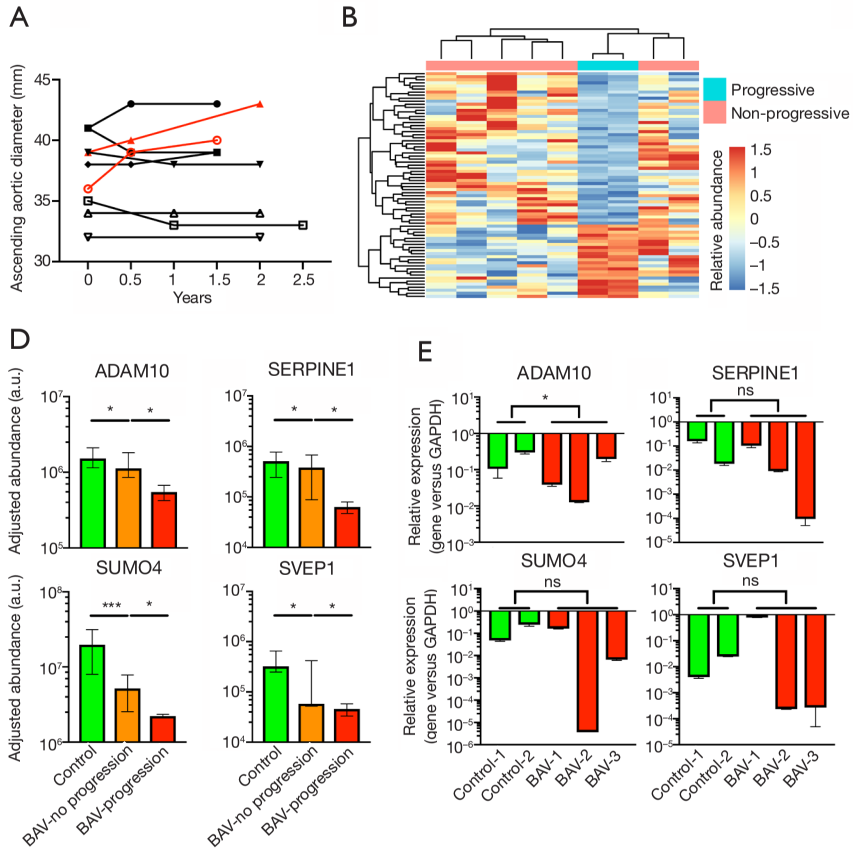

Protein	Uniprot ID	Molecular functions	Biological processes
ADAM10	O14672	hydrolase, metalloprotease, protease	notch signaling pathway
APOC2	P02655	lipid binding, lipase inhibitor activity, phospholipase binding	lipid degradation, lipid metabolism, lipid transport
APOC4	P55056	lipid transporter activity	lipid transport, transport
ERP44	Q9BS26	chaperone	stress response
MAN2A1	Q16706	glycosidase, hydrolase	protein glycosylation, N-glycan processing, protein deglycosylation
MED30	Q96HR3	nuclear receptor transcription coactivator activity, transcription coregulator activity	transcription, transcription regulation
SERPINE1	P05121	protease inhibitor, serine protease inhibitor	angiogenesis, dentinogenesis, positive regulation of odontoblast differentiation
SH3BGRL2	Q9UJC5	sh3 domain binding	-
SUMO4	Q6EEV6	protein tag, ubiquitin-like protein ligase binding	cellular response to oxidative stress, protein sumoylation
SVEP1	Q4LDE5	calcium ion binding	cell adhesion
UMOD	P07911	extracellular matrix structural constituent	leukocyte cell-cell adhesion, neutrophil migration

Figure 4 Comparative proteomic analysis of plasma proteins in stenotic BAV patients with and without progressive aortic dilation. (A) Follow-up measurement of the ascending aortic diameter showing rapid progression in two patients (labeled red). (B) Overall heatmap and dendrogram of the DEPs between the two subgroups of BAV patients. (C,D) List of the overlapped DEPs between BAV patients and controls and between BAV patients with and without progressive aortic dilation that exhibited similar trends. *ADAM10*, *SERPINE1*, *SUMO4*, and *SVEP1* are Notch signaling and aortic aneurysm-related proteins, the levels of which are lower in BAV patients without progression and further inhibited in those with rapid progression (n=3). (E,F) Downregulation of *ADAM10* in BAV aortic smooth muscle cells is observed by qRT-PCR, and *ADAM10* concentration is slightly decreased in the culture supernatant of the diseased cells (n=3). Values are presented as median and interquartile range. ns, not significant, *P<0.05, and ***P<0.001. BAV, bicuspid aortic valve; DEPs, differentially expressed proteins.

modifier 4 (*SUMO4*), and sushi, von Willebrand factor type A, EGF and pentraxin domain containing 1 (*SVEP1*), were downregulated in BAV patients and further inhibited in those with progressive aortic dilation (*Figure 4D*). Transcription of the *ADAM10* gene was consistently downregulated in BAV aortic smooth muscle cells, while other proteins did not show a similar trend (*Figure 4E*). The concentration of *ADAM10* was higher in the supernatant of control cells, although the difference did not quite reach the threshold of statistical significance (P=0.073; *Figure 4F*).

Discussion

BAV-related aortic dilation is a complicated disease associated with genetic mutations and aberrant hemodynamics (1). To date, the molecular mechanism of aortic disease in patients with BAV remains unclear. In this study, proteomic analysis showed that patients with a stenotic BAV had plasma protein profiles distinct from those of controls. Proteins abnormally expressed in thoracic aortic aneurysm tissues exhibited similar alterations in the plasma, indicating the potential of plasma biomarkers in predicting tissue pathologies. For instance, *NOTCH3* was relevant to the existing degree of aortic dilation (a static state), while the plasma level of *ADAM10* indicated rapidly progressive aortic dilation (a dynamic state). Our findings shed light on the distinct characteristics in the plasma proteome of BAV patients, which could be exploited to identify biomarkers that could predict disease progression or outcomes.

From a general perspective, the proteomic landscape of BAV patients' plasma differed significantly from that of healthy controls, which corresponded with the fact that aortic dilation in BAV patients may commence early in life, suggesting an intrinsic defect in this population (3). The identified DEPs between BAV patients and controls included several thoracic aortic aneurysm-related proteins, namely *COL1A1*, *FBN1*, *FLNA*, and *NOTCH3*. It is well established that mutations in *COL1A1*, *FBN1*, and *FLNA* cause familial thoracic aortic aneurysm (20,27-29), but in this study, the plasma levels of these proteins were not independently associated with the ascending aortic diameter. The Notch receptor family member *NOTCH1* is associated with BAV as well as thoracic aortic aneurysm (2,24). As an important interactor of *NOTCH1*, *NOTCH3* is also reported to promote protective remodeling pathways in vascular smooth muscle cells (24,30). In this study, we observed an independent correlation between the *NOTCH3* level and the ascending aortic diameter, and downregulation of *NOTCH3* and the Notch downstream effector *HEY2* in the diseased aortic smooth muscle cells, implying that systemic *NOTCH3* insufficiency in stenotic BAV patients might be traced to pathologies in the aorta.

Rapid progressive ascending aortic dilation commonly results in a higher risk of morbidity and mortality than stable dilation (4). Considering the high prevalence of BAV in the general population, the biological difference between patients with and without progressive aortic dilation is clinically meaningful and should be clarified. In this study, a subset of proteins was correlated with progressive aortic dilation. *ADAM10* is a metalloprotease that controls the proteolytic processing of Notch receptors: Whilst insufficiency in expression of Notch receptors results in lower levels of the Notch intracellular domain in the cytoplasm and transcriptional activation of Notch target genes, downregulation of *ADAM10* may block the liberation of the Notch intracellular domain, further impairing Notch signaling (22). Consistently, we observed downregulation of *ADAM10* in aortic smooth muscle cells. Other top-hit proteins, namely *SERPINE1*, *SUMO4*, and *SVEP1*, were also associated with progressive aortic dilation but were not evidently downregulated in aortic smooth muscle cells. This discrepancy could be explained by the fact that the plasma protein network arises partly via systemic cross-tissue regulations. A follow-up validation of these primary data is warranted to adjust for bias derived from other tissues and organs (31). Moreover, the type and degree of valvular dysfunction may also contribute to the pattern of aortic dilation (1). Future studies may also include more patients with multiple valve configurations to provide a comprehensive landscape of BAV plasma proteomics. Although our study only included patients with stenotic BAV, this proteomics method can be applied to other causes of thoracic aortic aneurysm, namely sporadic (tricuspid) and Marfan cases.

In conclusion, the current study is the first to profile plasma proteomics in patients with a stenotic BAV. The potential for plasma proteins such as *NOTCH3* and *ADAM10* to predict aortic dilation is also proposed, which merits further mechanistic and clinical investigations.

Acknowledgments

The authors thank Hangqi Shen, MD, PhD, Shanghai Jiao Tong University, for her support in manuscript preparation.

Funding: This work was supported by grants from the National Natural Science Foundation of China (81771971, 82070482, 81772007, and 82070484), the Science and Technology Commission of Shanghai Municipality (20ZR1411700), and the Shanghai Municipal Science and Technology Major Project (2017SHZDZX01).

Footnote

Reporting Checklist: The authors have completed the MDAR reporting checklist. Available at https://dx.doi.org/10.21037/atm-21-3378

Data Sharing Statement: Available at https://dx.doi.org/10.21037/atm-21-3378

Conflicts of Interest: All authors have completed the ICMJE uniform disclosure form (available at https://dx.doi.org/10.21037/atm-21-3378). The authors have no conflicts of interest to declare.

Ethical Statement: The authors are accountable for all aspects of the work in ensuring that questions related to the accuracy or integrity of any part of the work are appropriately investigated and resolved. All procedures performed in this study involving human participants were in accordance with the Declaration of Helsinki (as revised in 2013). This study was approved by Zhongshan Hospital Fudan University Ethics Committee (Approval Letter No. B2020-158R), and written consent was obtained from all study subjects.

References

1. Verma S, Siu SC. Aortic dilatation in patients with bicuspid aortic valve. N Engl J Med 2014;370:1920-9.
2. Bob-Manuel T, Heckle MR, Ifedili IA, et al. Outcomes of transcatheter aortic valve replacement in bicuspid aortic valve stenosis. Ann Transl Med 2019;7:102.
3. Grattan M, Prince A, Rumman RK, et al. Predictors of Bicuspid Aortic Valve-Associated Aortopathy in Childhood: A Report From the MIBAVA Consortium. Circ Cardiovasc Imaging 2020;13:e009717.
4. Borger MA, Fedak PWM, Stephens EH, et al. The American Association for Thoracic Surgery consensus guidelines on bicuspid aortic valve-related aortopathy: Full online-only version. J Thorac Cardiovasc Surg 2018;156:e41-74.
5. Lo Presti F, Guzzardi DG, Bancone C, et al. The science of BAV aortopathy. Prog Cardiovasc Dis 2020;63:465-74.
6. Pasipoularides A. Clinical-pathological correlations of BAV and the attendant thoracic aortopathies. Part 1: Pluridisciplinary perspective on their hemodynamics and morphomechanics. J Mol Cell Cardiol 2019;133:223-32.
7. Abdulkareem N, Soppa G, Jones S, et al. Dilatation of the remaining aorta after aortic valve or aortic root replacement in patients with bicuspid aortic valve: a 5-year follow-up. Ann Thorac Surg 2013;96:43-9.
8. Yasuda H, Nakatani S, Stugaard M, et al. Failure to prevent progressive dilation of ascending aorta by aortic valve replacement in patients with bicuspid aortic valve: comparison with tricuspid aortic valve. Circulation 2003;108 Suppl 1:II291-4.
9. Lee R, Cassimee I, Huang H, et al. Integrated Plasma and Tissue Proteomics Reveals Attractin Release by Intraluminal Thrombus of Abdominal Aortic Aneurysms and Improves Aneurysm Growth Prediction in Humans. Ann Surg 2020. [Epub ahead of print]. doi: 10.1097/SLA.0000000000004439.
10. Pasta S, Agnese V, Gallo A, et al. Shear Stress and Aortic Strain Associations With Biomarkers of Ascending Thoracic Aortic Aneurysm. Ann Thorac Surg 2020;110:1595-604.
11. Huang J, Cheng L, Li J, et al. Myocardin regulates expression of contractile genes in smooth muscle cells and is required for closure of the ductus arteriosus in mice. J Clin Invest 2008;118:515-25.
12. McCarthy DJ, Chen Y, Smyth GK. Differential expression analysis of multifactor RNA-Seq experiments with respect to biological variation. Nucleic Acids Res 2012;40:4288-97.
13. Robinson MD, McCarthy DJ, Smyth GK. edgeR: a Bioconductor package for differential expression analysis of digital gene expression data. Bioinformatics 2010;26:139-40.
14. Ritchie ME, Phipson B, Wu D, et al. limma powers

differential expression analyses for RNA-sequencing and microarray studies. Nucleic Acids Res 2015;43:e47.
15. Zhou Y, Zhou B, Pache L, et al. Metascape provides a biologist-oriented resource for the analysis of systems-level datasets. Nat Commun 2019;10:1523.
16. Ashburner M, Ball CA, Blake JA, et al. Gene ontology: tool for the unification of biology. The Gene Ontology Consortium. Nat Genet 2000;25:25-9.
17. Gene Ontology Consortium. The Gene Ontology resource: enriching a GOld mine. Nucleic Acids Res 2021;49:D325-34.
18. Szklarczyk D, Gable AL, Lyon D, et al. STRING v11: protein-protein association networks with increased coverage, supporting functional discovery in genome-wide experimental datasets. Nucleic Acids Res 2019;47:D607-13.
19. Bossone E, Eagle KA. Epidemiology and management of aortic disease: aortic aneurysms and acute aortic syndromes. Nat Rev Cardiol 2021;18:331-48.
20. Ziganshin BA, Bailey AE, Coons C, et al. Routine Genetic Testing for Thoracic Aortic Aneurysm and Dissection in a Clinical Setting. Ann Thorac Surg 2015;100:1604-11.
21. Elefteriades JA, Pomianowski P. Practical genetics of thoracic aortic aneurysm. Prog Cardiovasc Dis 2013;56:57-67.
22. Alabi RO, Farber G, Blobel CP. Intriguing Roles for Endothelial ADAM10/Notch Signaling in the Development of Organ-Specific Vascular Beds. Physiol Rev 2018;98:2025-61.
23. Koenig SN, LaHaye S, Feller JD, et al. Notch1 haploinsufficiency causes ascending aortic aneurysms in mice. JCI Insight 2017;2:e91353.
24. Garg V, Muth AN, Ransom JF, et al. Mutations in NOTCH1 cause aortic valve disease. Nature 2005;437:270-4.
25. Yassine NM, Shahram JT, Body SC. Pathogenic Mechanisms of Bicuspid Aortic Valve Aortopathy. Front Physiol 2017;8:687.
26. Meester JAN, Verstraeten A, Alaerts M, et al. Overlapping but distinct roles for NOTCH receptors in human cardiovascular disease. Clin Genet 2019;95:85-94.
27. Isselbacher EM, Lino Cardenas CL, Lindsay ME. Hereditary Influence in Thoracic Aortic Aneurysm and Dissection. Circulation 2016;133:2516-28.
28. Crosas-Molist E, Meirelles T, López-Luque J, et al. Vascular smooth muscle cell phenotypic changes in patients with Marfan syndrome. Arterioscler Thromb Vasc Biol 2015;35:960-72.
29. Chen MH, Choudhury S, Hirata M, et al. Thoracic aortic aneurysm in patients with loss of function Filamin A mutations: Clinical characterization, genetics, and recommendations. Am J Med Genet A 2018;176:337-50.
30. Biros E, Walker PJ, Nataatmadja M, et al. Downregulation of transforming growth factor, beta receptor 2 and Notch signaling pathway in human abdominal aortic aneurysm. Atherosclerosis 2012;221:383-6.
31. Emilsson V, Ilkov M, Lamb JR, et al. Co-regulatory networks of human serum proteins link genetics to disease. Science 2018;361:769-73.

(English Language Editor: D. Fitzgerald)

Cite this article as: Ma W, Zhang J, Xu K, Yan S, Liu D, Huang H, Tang Y, Yan G, Sun Y, Li J, Zhang W, Wang C, Zhu K, Lai H. Plasma proteomic profiling reveals biomarkers associated with aortic dilation in patients with bicuspid aortic valve. Ann Transl Med 2021;9(14):1182. doi: 10.21037/atm-21-3378

Supplementary

Table S1 Baseline characteristics of the included BAV patients and healthy controls

Demographics	BAV patients (n=30)	Healthy controls (n=15)	P value
Age (years)	54.1±13.1	51.1±7.0	0.403[a]
Male gender	15 (50.0)	12 (80.0)	0.063[b]
Hypertension	10 (33.3)	0 (0)	0.019[b]
Diabetes	1 (0.3)	0 (0)	>0.999[b]
Coronary artery disease	2 (0.7)	0 (0)	0.545[b]
Hyperlipidemia	2 (0.7)	0 (0)	0.545[b]
History of smoking	8 (26.7)	2 (13.3)	0.456[b]
Ascending aortic diameter (mm)	43.9±6.9	31.8±2.2	<0.001[a]
Ascending aortic diameter ≥45 mm	17 (56.7)	0 (0)	<0.001[b]
Severity of aortic stenosis			<0.001[c]
Mild	2 (6.7)	0 (0)	
Moderate	7 (23.3)	0 (0)	
Severe	21 (70.0)	0 (0)	

Continuous variables are expressed as means ± standard deviations, and categorical variables as numbers (percentages). Data are compared using [a]Student's t-test, [b]Fisher's exact test, and [c]Cochran-Mantel-Haenszel test. BAV, bicuspid aortic valve.

Table S2 Baseline characteristics of the patients from whom the aortic smooth muscle cells were harvested

Patients	Age (year)	Gender	Hypertension	Ascending aortic diameter (mm)	Aortic stenosis
Control-1	38	Female	No	N/A	No
Control-2	22	Male	No	N/A	No
BAV-1	50	Female	No	43	Severe
BAV-2	46	Male	Yes	53	Severe
BAV-3	74	Male	Yes	53	Severe

BAV, bicuspid aortic valve.

https://dx.doi.org/10.21037/atm-21-3378

Table S3 DEPs between BAV patients and healthy controls using cutoff values of P<0.05 and fold-change ratio >1.5

logFC	AveExpr	t	P.Value	adj.P.Val	B	UNIPROT	Gene name
2.767056	23.70452	3.008633	0.004247	0.022369	–2.51371	P20742	*PZP*
2.628587	23.89302	5.256278	3.70E–06	9.55E–05	4.167766	Q9P2P1	*NYNRIN*
2.620848	19.26652	7.382316	2.44E–09	3.04E–07	11.26183	P07602	*PSAP*
2.326093	24.50175	6.706861	2.51E–08	1.56E–06	9.00065	P59666	*DEFA3*
1.821323	18.34192	6.975828	9.90E–09	1.06E–06	9.902823	Q6UY14	*ADAMTSL4*
1.781201	17.69439	7.788113	6.08E–10	1.14E–07	12.60953	Q8WZ42	*TTN*
1.740143	20.04425	6.785227	1.91E–08	1.30E–06	9.263643	P0DMV9	*HSPA1B*
1.668907	17.62123	5.757642	6.67E–07	2.38E–05	5.822482	Q07954	*LRP1*
1.625418	22.24402	5.873392	4.48E–07	1.86E–05	6.207936	Q8NBJ4	*GOLM1*
1.577001	20.68018	5.577753	1.24E–06	4.21E–05	5.225652	P07237	*P4HB*
1.531367	21.56249	4.959956	1.01E–05	0.000228	3.205701	P63241	*EIF5A*
1.525534	21.61898	8.305536	1.05E–10	3.01E–08	14.30949	P40925	*MDH1*
1.504118	20.60417	8.264965	1.21E–10	3.01E–08	14.17707	P04179	*SOD2*
1.446448	21.18032	6.859462	1.48E–08	1.20E–06	9.512687	O15511	*ARPC5*
1.434917	20.59583	5.983239	3.07E–07	1.43E–05	6.574571	P14314	*PRKCSH*
1.413736	21.89214	4.452534	5.37E–05	0.000855	1.598457	O15143	*ARPC1B*
1.383253	19.35201	4.002136	0.000226	0.002731	0.229096	P16109	*SELP*
1.355334	18.20865	3.483163	0.001098	0.009255	–1.25935	P02452	*COL1A1*
1.343613	20.96687	3.208893	0.002429	0.015141	–1.9983	O15144	*ARPC2*
1.335867	21.95904	6.11232	1.96E–07	1.05E–05	7.00626	P80188	*LCN2*
1.32445	17.94713	2.89298	0.005813	0.028606	–2.80131	P11216	*PYGB*
1.306756	19.73355	2.736812	0.008788	0.037139	–3.17724	P62873	*GNB1*
1.276435	18.91974	3.180461	0.002632	0.015811	–2.07277	Q9NZK5	*ADA2*
1.273504	21.82659	3.24801	0.002173	0.014014	–1.89517	O15037	*KHNYN*
1.244134	20.18369	4.280279	9.37E–05	0.001323	1.06744	Q86U17	*SERPINA11*
1.230921	19.33215	4.24268	0.000106	0.001464	0.952675	P24821	*TNC*
1.213669	23.9209	5.105618	6.16E–06	0.000154	3.676816	O95810	*CAVIN2*
1.202976	18.60707	4.912257	1.18E–05	0.000259	3.052263	P48637	*GSS*
1.197772	19.5404	3.947472	0.000268	0.002997	0.067391	Q9Y5C1	*ANGPTL3*
1.1814	21.86502	5.90132	4.07E–07	1.79E–05	6.301078	P18669	*PGAM1*
1.158584	19.44166	2.867433	0.006225	0.029284	–2.8638	P36871	*PGM1*
1.152961	18.34589	4.311577	8.48E–05	0.001219	1.163292	Q16706	*MAN2A1*
1.136316	18.14065	2.964793	0.004787	0.024525	–2.62363	P22897	*MRC1*
1.119627	17.90809	3.114158	0.003171	0.017834	–2.2448	P29350	*PTPN6*
1.114146	21.15054	4.466956	5.13E–05	0.000834	1.643291	P52209	*PGD*
1.100415	21.5133	5.29247	3.27E–06	8.97E–05	4.286204	P50395	*GDI2*
1.095313	18.11763	4.350417	7.48E–05	0.001119	1.282638	P08758	*ANXA5*
1.09237	18.88366	4.103652	0.000164	0.002085	0.532145	Q9H4A9	*DPEP2*
1.072839	19.86737	3.402571	0.001391	0.01062	–1.48023	P51149	*RAB7A*
1.065709	17.47763	3.974212	0.000247	0.002842	0.146358	P07942	*LAMB1*
1.003138	21.14033	4.127838	0.000152	0.001999	0.604856	Q04917	*YWHAH*
0.998304	19.06763	2.30747	0.02558	0.080393	–4.1308	P05067	*APP*
0.972807	21.38062	3.332812	0.001704	0.01219	–1.66895	O15145	*ARPC3*

0.968451	23.04386	5.070737	6.93E–06	0.000167	3.563667	P31146	*CORO1A*
0.967585	17.72127	3.126464	0.003064	0.017361	–2.21304	P22314	*UBA1*
0.967195	23.10594	5.988343	3.01E–07	1.43E–05	6.591626	P26038	*MSN*
0.964596	20.40342	2.783331	0.00778	0.033836	–3.0668	P55072	*VCP*
0.942494	18.14881	2.885752	0.005927	0.028751	–2.81903	Q07960	*ARHGAP1*
0.937264	18.75228	3.478534	0.001114	0.009255	–1.27212	P40189	*IL6ST*
0.921912	26.92135	4.343473	7.65E–05	0.001122	1.261272	P02671	*FGA*
0.918051	20.36725	2.899247	0.005716	0.028314	–2.78592	Q14847	*LASP1*
0.916045	19.98295	4.769317	1.90E–05	0.000384	2.595146	Q9BY67	*CADM1*
0.91168	25.42008	3.464393	0.001161	0.009543	–1.31106	Q9BXR6	*CFHR5*
0.911158	19.97956	2.879318	0.00603	0.028751	–2.83478	P31150	*GDI1*
0.905598	20.76018	3.51109	0.001011	0.008763	–1.18212	P29401	*TKT*
0.879173	22.29589	2.867647	0.006221	0.029284	–2.86328	Q9ULV4	*CORO1C*
0.871934	22.81204	6.166436	1.63E–07	9.37E–06	7.187463	Q99497	*PARK7*
0.869974	23.75752	4.722391	2.22E–05	0.000425	2.446018	P08637	*FCGR3A*
0.857112	20.5012	3.108323	0.003223	0.017916	–2.25982	P07384	*CAPN1*
0.848499	23.88176	2.39104	0.020948	0.069028	–3.95491	P62979	*RPS27A*
0.831939	19.43033	2.458389	0.017781	0.060731	–3.80964	Q9Y696	*CLIC4*
0.831847	19.13566	2.591887	0.01275	0.049673	–3.51268	P07307	*ASGR2*
0.831545	18.10959	2.197487	0.033059	0.097984	–4.35471	P07911	*UMOD*
0.827684	21.20568	2.343397	0.023487	0.075724	–4.05578	Q9Y2K3	*MYH15*
0.819518	18.53301	2.403387	0.020332	0.067593	–3.92851	O43396	*TXNL1*
0.816386	23.23592	2.81119	0.007229	0.032575	–3.00002	Q92686	*NRGN*
0.809804	19.98158	2.188888	0.033718	0.099258	–4.37184	Q7Z7G0	*ABI3BP*
0.808821	18.19872	3.31974	0.001769	0.012368	–1.70405	P10619	*CTSA*
0.806301	23.3074	3.179156	0.002642	0.015811	–2.07618	P60709	*ACTB*
0.794206	20.13511	3.283499	0.001964	0.012998	–1.80093	P09493	*TPM1*
0.785136	19.71834	3.35652	0.001591	0.011782	–1.60507	P06576	*ATP5F1B*
0.765696	21.31632	2.91681	0.005452	0.027368	–2.74268	P68036	*UBE2L3*
0.743636	22.49809	3.535293	0.000941	0.008508	–1.1149	Q15942	*ZYX*
0.742917	21.5304	2.419202	0.019567	0.065339	–3.89455	Q92496	*CFHR4*
0.737743	26.19028	3.594723	0.000789	0.007402	–0.94875	P37802	*TAGLN2*
0.735802	26.77309	4.560714	3.77E–05	0.000642	1.936072	P19652	*ORM2*
0.726218	22.70613	4.182818	0.000128	0.00174	0.770853	P22392	*NME2*
0.722578	19.42471	2.355916	0.022794	0.07448	–4.02943	P54289	*CACNA2D1*
0.717511	22.65345	3.209774	0.002423	0.015141	–1.99599	Q3ZCW2	*LGALSL*
0.706609	18.52895	2.747383	0.008549	0.036542	–3.15226	P16152	*CBR1*
0.700815	26.00444	2.670776	0.010427	0.042388	–3.33173	P02675	*FGB*
0.700047	26.09667	2.700721	0.009652	0.040109	–3.26202	P02679	*FGG*
0.699753	19.04766	2.124067	0.039072	0.108646	–4.49926	P49721	*PSMB2*
0.69882	23.53883	3.620495	0.00073	0.007	–0.87622	P78417	*GSTO1*
0.695439	18.9113	2.496297	0.016195	0.059078	–3.72652	Q9NY97	*B3GNT2*
0.691181	18.62286	2.059213	0.04516	0.120216	–4.6236	Q16851	*UGP2*
0.68586	21.72962	2.423178	0.019378	0.065	–3.88598	Q15555	*MAPRE2*
0.683538	19.73187	2.132891	0.038302	0.108468	–4.4821	P17174	*GOT1*
0.681045	21.99428	3.534363	0.000944	0.008508	–1.11749	P61158	*ACTR3*
0.674793	18.95101	2.156041	0.036344	0.104159	–4.4368	Q9UEW3	*MARCO*
0.662929	22.62578	3.095966	0.003336	0.018214	–2.29159	P21926	*CD9*
0.660237	17.99514	2.63897	0.011312	0.044771	–3.40517	Q9UQ80	*PA2G4*
0.659068	21.20019	2.694965	0.009797	0.040485	–3.27546	P37837	*TALDO1*

0.640482	21.61244	2.119224	0.0395	0.10943	–4.50866	P61160	*ACTR2*
0.633471	20.83872	2.84901	0.006539	0.030191	–2.90863	Q8NBP7	*PCSK9*
0.627065	23.93667	3.340123	0.001668	0.012114	–1.64928	P27797	*CALR*
0.619891	24.00249	2.508425	0.015716	0.058194	–3.69972	Q02985	*CFHR3*
0.619094	23.17463	3.579187	0.000826	0.007628	–0.99233	P62258	*YWHAE*
0.612037	21.75361	3.155757	0.002822	0.016588	–2.13714	P99999	*CYCS*
0.59931	18.83744	2.092803	0.041911	0.114832	–4.5596	O75874	*IDH1*
0.595465	21.32069	2.506177	0.015803	0.058232	–3.7047	P06744	*GPI*
0.59379	22.67773	2.18733	0.033839	0.099258	–4.37494	P10124	*SRGN*
–0.58716	21.87824	–2.87903	0.006035	0.028751	–2.83548	P08493	*MGP*
–0.58849	18.70042	–2.30208	0.025908	0.080745	–4.14198	O00194	*RAB27B*
–0.58932	27.74555	–3.10717	0.003233	0.017916	–2.26278	O75636	*FCN3*
–0.59167	21.25995	–2.90088	0.005691	0.028314	–2.78191	O75144	*ICOSLG*
–0.59196	18.7551	–2.29254	0.026497	0.08224	–4.1617	P35590	*TIE1*
–0.59801	20.68082	–2.51436	0.015486	0.057628	–3.68658	A0A075B6H9	*IGLV4–69*
–0.59855	27.78072	–4.60247	3.29E–05	0.000597	2.067192	P29622	*SERPINA4*
–0.6164	18.06488	–2.7871	0.007704	0.033698	–3.05779	P30085	*CMPK1*
–0.61804	19.69274	–3.44969	0.001212	0.009856	–1.35145	Q9ULI3	*HEG1*
–0.62678	19.32313	–2.31836	0.024928	0.079685	–4.10816	Q96HR3	*MED30*
–0.62733	19.11292	–2.17555	0.034763	0.101179	–4.39831	P24666	*ACP1*
–0.62896	18.24661	–2.15658	0.0363	0.104159	–4.43575	P35237	*SERPINB6*
–0.63872	30.22683	–3.25388	0.002137	0.013901	–1.87963	P02656	*APOC3*
–0.6389	18.76625	–2.30393	0.025795	0.08073	–4.13814	Q15185	*PTGES3*
–0.64104	32.99921	–5.53509	1.43E–06	4.66E–05	5.084573	P02766	*TTR*
–0.645	20.84826	–2.55222	0.014089	0.053769	–3.60214	Q9UJJ9	*GNPTG*
–0.6547	21.39109	–3.80408	0.000418	0.004405	–0.35156	Q14515	*SPARCL1*
–0.665	18.11266	–2.10879	0.040437	0.111612	–4.52883	Q9BS26	*ERP44*
–0.66778	21.61836	–2.09333	0.041861	0.114832	–4.55858	P48059	*LIMS1*
–0.6922	20.12897	–2.35388	0.022906	0.07448	–4.03373	O14672	*ADAM10*
–0.69248	20.61653	–2.3131	0.025241	0.080304	–4.11911	O75368	*SH3BGRL*
–0.69401	23.68931	–4.59678	3.35E–05	0.000597	2.049282	Q9UHG3	*PCYOX1*
–0.70117	29.67334	–3.42459	0.001305	0.010273	–1.42018	P02655	*APOC2*
–0.71114	22.05195	–3.95284	0.000264	0.002992	0.083238	Q9UNW1	*MINPP1*
–0.71339	25.96284	–3.38063	0.001483	0.011207	–1.53983	P00915	*CA1*
–0.72801	23.35504	–2.05547	0.045536	0.120293	–4.63068	P21333	*FLNA*
–0.7382	18.22536	–2.44829	0.018227	0.061412	–3.83163	P42574	*CASP3*
–0.74297	25.2757	–4.65274	2.79E–05	0.000522	2.225565	Q96KN2	*CNDP1*
–0.75537	16.63084	–2.05993	0.045089	0.120216	–4.62224	P19021	*PAM*
–0.75806	18.1138	–2.07399	0.043705	0.118878	–4.59556	P10721	*KIT*
–0.76205	17.58065	–2.81313	0.007192	0.032575	–2.99536	P19022	*CDH2*
–0.76895	19.44371	–2.71986	0.009185	0.038596	–3.21716	Q9NPY3	*CD93*
–0.77617	19.6671	–3.19884	0.002499	0.01545	–2.02469	P54802	*NAGLU*
–0.7799	22.2517	–3.63235	0.000704	0.006843	–0.84275	P15151	*PVR*
–0.78798	19.69898	–3.91926	0.000293	0.003224	–0.01565	P59923	*ZNF445*
–0.7922	24.62023	–4.50295	4.56E–05	0.000758	1.755407	P32119	*PRDX2*
–0.79678	17.27914	–2.05252	0.045834	0.120293	–4.63626	Q86SQ4	*ADGRG6*
–0.81269	20.07022	–3.97576	0.000246	0.002842	0.150947	Q9UJC5	*SH3BGRL2*
–0.81343	20.83612	–3.47936	0.001111	0.009255	–1.26983	Q16270	*IGFBP7*
–0.83381	20.25724	–2.55946	0.013836	0.053346	–3.5859	P19105	*MYL12A*
–0.83528	19.93333	–4.11182	0.00016	0.002067	0.556675	O14960	*LECT2*

–0.85344	16.68609	–2.95009	0.004982	0.025351	–2.66024	P28827	*PTPRM*
–0.87867	22.89328	–7.69561	8.34E–10	1.25E–07	12.30331	Q99969	*RARRES2*
–0.88969	22.90117	–2.20126	0.032773	0.097984	–4.34717	P02792	*FTL*
–0.89363	20.27668	–2.62806	0.011632	0.045552	–3.43021	P01782	*IGHV3–9*
–0.90708	17.32458	–2.71243	0.009364	0.039128	–3.23461	Q12884	*FAP*
–0.91172	17.98793	–2.67643	0.010276	0.042004	–3.31861	P42785	*PRCP*
–0.9288	22.94436	–4.83802	1.51E–05	0.000323	2.814342	P24592	*IGFBP6*
–0.95702	19.52893	–2.97007	0.004719	0.024342	–2.61046	P55083	*MFAP4*
–0.97686	17.48065	–3.29467	0.001902	0.012841	–1.77114	P16112	*ACAN*
–0.98064	19.16312	–2.81726	0.007114	0.032447	–2.98542	Q13642	*FHL1*
–0.99253	17.61818	–2.47996	0.016862	0.060349	–3.76246	P06737	*PYGL*
–1.00739	21.52836	–2.46804	0.017364	0.060645	–3.78856	P68366	*TUBA4A*
–1.02362	18.96996	–2.92173	0.00538	0.02719	–2.73053	P13489	*RNH1*
–1.02713	18.67781	–2.80237	0.0074	0.032758	–3.02122	O43895	*XPNPEP2*
–1.03453	18.39688	–4.14238	0.000146	0.001943	0.648677	Q9Y577	*TRIM17*
–1.05029	18.0229	–2.53107	0.014855	0.056118	–3.64944	P05121	*SERPINE1*
–1.06517	18.28666	–4.05892	0.000189	0.002361	0.39819	Q14118	*DAG1*
–1.08525	17.74421	–2.99168	0.004448	0.023269	–2.55635	Q14012	*CAMK1*
–1.10347	16.7497	–2.28046	0.027261	0.083571	–4.18659	Q96KP4	*CNDP2*
–1.10432	20.55709	–3.34478	0.001646	0.01207	–1.63675	P04439	*HLA–A*
–1.10522	20.17512	–3.74289	0.000504	0.005178	–0.52797	P68363	*TUBA1B*
–1.11056	16.85619	–2.76733	0.008114	0.035084	–3.10494	P05164	*MPO*
–1.1198	20.86017	–3.74212	0.000505	0.005178	–0.53016	Q96S96	*PEBP4*
–1.1363	18.39763	–2.13783	0.037876	0.107724	–4.47247	P78371	*CCT2*
–1.1649	18.16174	–2.21825	0.031514	0.094669	–4.31311	P35555	*FBN1*
–1.19348	19.47393	–4.81094	1.65E–05	0.000343	2.727823	P25774	*CTSS*
–1.22895	20.59661	–3.3272	0.001732	0.012219	–1.68403	A0A0C4DH67	*IGKV1–8*
–1.25372	16.31878	–2.87987	0.006021	0.028751	–2.83343	Q9UM47	*NOTCH3*
–1.29606	20.91207	–3.04805	0.00381	0.020356	–2.41398	P58546	*MTPN*
–1.34843	21.94354	–3.14432	0.002914	0.016881	–2.16682	P05062	*ALDOB*
–1.3514	17.39731	–3.90995	0.000302	0.00327	–0.04298	P07686	*HEXB*
–1.39663	19.91201	–3.98579	0.000238	0.002828	0.180635	P35579	*MYH9*
–1.41771	17.74486	–4.39116	6.56E–05	0.001022	1.408298	P61026	*RAB10*
–1.47176	25.99733	–6.83656	1.60E–08	1.20E–06	9.435853	P55056	*APOC4*
–1.53603	16.94818	–3.29336	0.001909	0.012841	–1.77463	P20929	*NEB*
–1.62705	18.6041	–5.80589	5.65E–07	2.11E–05	5.983017	P53004	*BLVRA*
–1.66419	16.55831	–3.7094	0.000558	0.005567	–0.62387	P49641	*MAN2A2*
–1.66656	17.18524	–3.33131	0.001711	0.01219	–1.67298	Q4LDE5	*SVEP1*
–1.73324	17.32028	–5.02932	7.97E–06	0.000186	3.429576	Q8TER0	*SNED1*
–1.73906	22.62501	–6.93045	1.16E–08	1.08E–06	9.750734	Q6UX06	*OLFM4*
–1.74071	17.55958	–2.97619	0.004641	0.024105	–2.59516	P78509	*RELN*
–1.80245	20.42949	–3.2357	0.002251	0.01439	–1.9277	Q8NF91	*SYNE1*
–1.84264	21.10424	–3.71486	0.000549	0.005549	–0.60826	O95497	*VNN1*
–1.98598	18.72425	–5.48764	1.68E–06	5.25E–05	4.927858	P27105	*STOM*
–2.02332	16.91737	–5.28644	3.34E–06	8.97E–05	4.266473	P49588	*AARS1*
–2.05286	18.26375	–4.37966	6.80E–05	0.001039	1.372776	Q7L591	*DOK3*
–2.14257	22.53984	–9.06389	8.42E–12	6.30E–09	16.7531	Q6EEV6	*SUMO4*
–2.14698	21.18986	–2.53182	0.014827	0.056118	–3.64776	O43852	*CALU*
–2.34615	23.44489	–3.5085	0.001019	0.008763	–1.18928	Q96NZ9	*PRAP1*
–3.35994	21.75497	–4.74802	2.04E–05	0.000401	2.527418	P84077	*ARF1*

DEPs, differentially expressed proteins; BAV, bicuspid aortic valve.

© Annals of Translational Medicine. All rights reserved.
https://dx.doi.org/10.21037/atm-21-3378

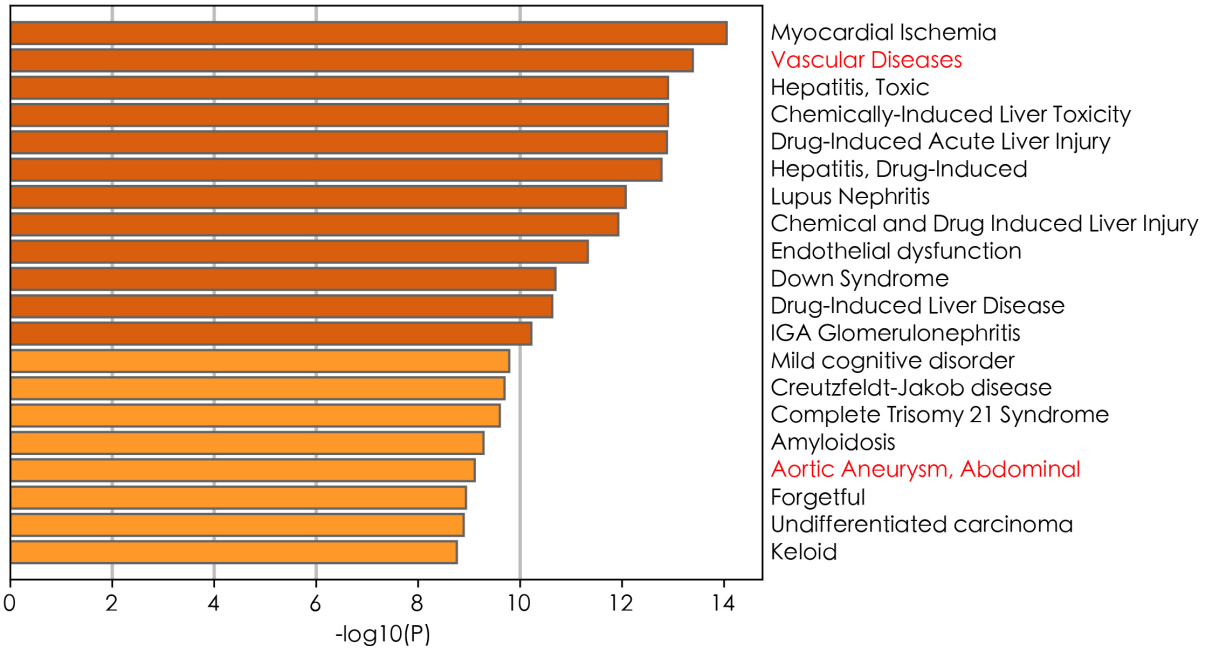

Figure S1 Disease enrichment analysis of the DEPs between BAV patients and controls. Cardiovascular diseases such as vascular diseases and abdominal aortic aneurysm (labeled red) are highly enriched. DEPs, differentially expressed proteins; BAV, bicuspid aortic valve.

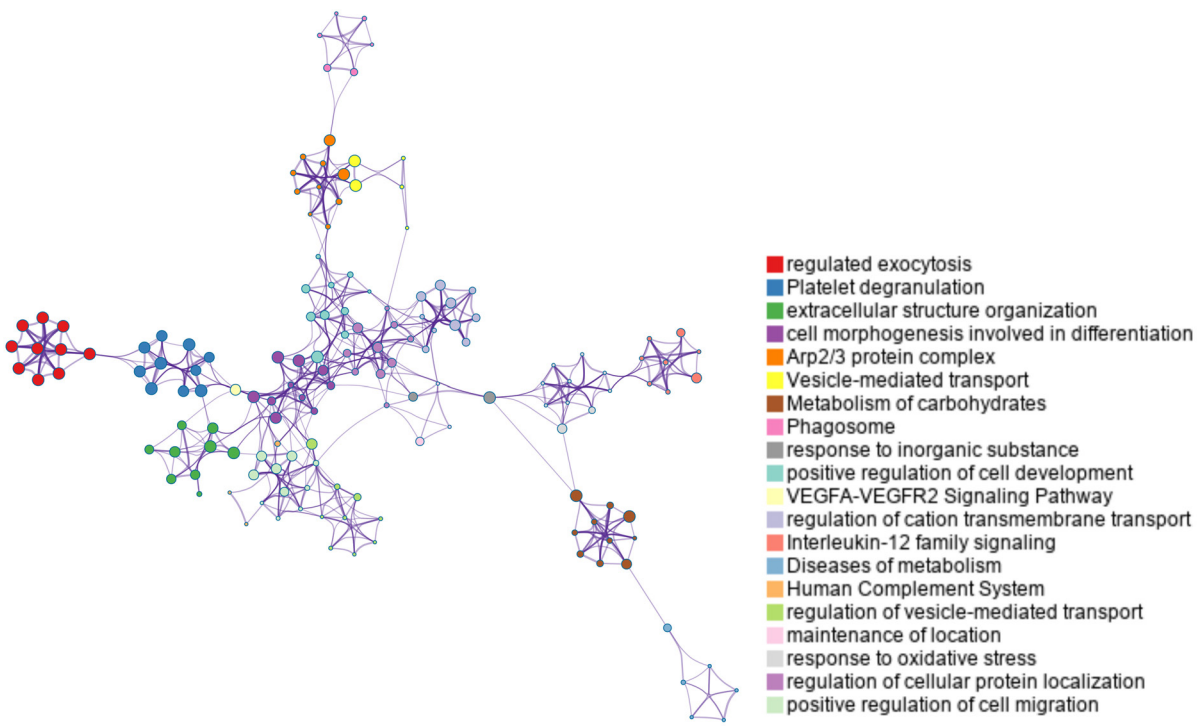

Figure S2 The top 20 clusters of the enriched biological processes of the DEPs between BAV patients and control. DEPs, differentially expressed proteins; BAV, bicuspid aortic valve.

https://dx.doi.org/10.21037/atm-21-3378

Table S4 DEPs between BAV patients with and without progressive aortic dilation using cutoff values of P<0.05 and fold-change ratio >1.5

P value	logFC	Adjust P value	UNIPROT	Gene name
0.023843	-0.78052	0.375216	A0A075B6K4	*IGLV3-10*
0.007486	-1.77323	0.294705	A0A0J9YXX1	*IGHV5-10-1*
0.015418	0.391122	0.365986	O00533	*CHL1*
0.017985	-1.40035	0.365986	O14672	*ADAM10*
0.005385	-2.06706	0.260209	O43488	*AKR7A2*
0.002163	1.22667	0.257634	O43493	*TGOLN2*
0.010086	1.664424	0.328	O43852	*CALU*
0.018944	1.0609	0.366444	O76074	*PDE5A*
0.03157	-0.57577	0.390214	P00441	*SOD1*
0.020188	-0.54302	0.366444	P00533	*EGFR*
0.049681	-0.32422	0.502177	P00568	*AK1*
0.005015	-0.58994	0.260209	P00740	*F9*
0.00932	-0.19366	0.316878	P00742	*F10*
0.000971	0.304493	0.242217	P01008	*SERPINC1*
0.021269	-0.37487	0.366444	P01031	*C5*
0.029746	-1.04776	0.390214	P01876	*IGHA1*
0.03172	-0.8792	0.390214	P02655	*APOC2*
0.002227	-2.45432	0.257634	P02741	*CRP*
0.035287	-0.42657	0.410234	P02753	*RBP4*
0.000256	0.508344	0.191618	P05090	*APOD*
0.028416	-2.59689	0.390214	P05121	*SERPINE1*
0.005419	-0.36726	0.260209	P05156	*CFI*
0.017291	-0.48839	0.365986	P07357	*C8A*
0.005568	1.556691	0.260209	P07911	*UMOD*
0.026802	0.436539	0.384033	P08185	*SERPINA6*
0.000635	-3.24178	0.237391	P09972	*ALDOC*
0.026296	-0.56556	0.384033	P0C0L4	*C4A*
0.017998	1.462011	0.365986	P10321	*HLA-C*
0.02168	-1.16282	0.366444	P10644	*PRKAR1A*
0.0031	0.686498	0.257634	P10646	*TFPI*
0.036714	-2.05085	0.410234	P13224	*GP1BB*
0.033175	0.678009	0.400237	P13716	*ALAD*
0.020199	0.772203	0.366444	P16112	*ACAN*
0.036097	-1.69914	0.410234	P20023	*CR2*
0.04191	0.774869	0.454324	P41240	*CSK*
0.029134	-1.58522	0.390214	P48426	*PIP4K2A*
0.027211	-0.56463	0.384033	P48637	*GSS*
0.02432	-1.90319	0.375216	P49407	*ARRB1*
0.011427	-0.47361	0.356128	P51149	*RAB7A*
0.014439	0.561058	0.365986	P51884	*LUM*
0.008061	0.913406	0.301471	P54802	*NAGLU*
0.008881	-1.92216	0.316316	P54819	*AK2*
0.013363	-1.41434	0.365986	P55056	*APOC4*
0.018104	-1.13536	0.365986	P61088	*UBE2N*
0.044376	-0.638	0.474189	P61916	*NPC2*
0.046453	-0.86744	0.482101	P62942	*FKBP1A*
0.006589	-0.30224	0.273802	P62979	*RPS27A*
0.013144	0.63441	0.365986	Q12860	*CNTN1*
0.005392	-1.72557	0.260209	Q14141	*SEPTIN6*
0.025081	-1.45493	0.375216	Q15019	*SEPTIN2*
0.020735	0.698228	0.366444	Q15166	*PON3*
0.037294	0.884489	0.410234	Q16706	*MAN2A1*
0.037136	-2.90432	0.410234	Q4LDE5	*SVEP1*
0.02485	-1.22303	0.375216	Q6EEV6	*SUMO4*
0.005914	1.008333	0.260209	Q76LX8	*ADAMTS13*
0.030199	0.852641	0.390214	Q7L591	*DOK3*
0.04705	0.741053	0.482101	Q86TH1	*ADAMTSL2*
0.046495	-0.89383	0.482101	Q8NBJ4	*GOLM1*
0.02245	0.743088	0.366444	Q92820	*GGH*
0.014649	-0.94753	0.365986	Q96HR3	*MED30*
0.017085	1.489395	0.365986	Q96NZ9	*PRAP1*
0.015545	-3.026	0.365986	Q99439	*CNN2*
0.030678	-2.25868	0.390214	Q99685	*MGLL*
0.003553	-1.2312	0.257634	Q9BR76	*CORO1B*
0.013768	-1.65934	0.365986	Q9BS26	*ERP44*
0.003369	-0.38306	0.257634	Q9BXR6	*CFHR5*
0.016244	-2.33835	0.365986	Q9HBB8	*CDHR5*
0.022535	-1.10941	0.366444	Q9HDC9	*APMAP*
0.034891	-1.40687	0.410234	Q9NZ08	*ERAP1*
0.020586	0.870296	0.366444	Q9UBQ6	*EXTL2*
0.001567	-1.17653	0.257634	Q9UJC5	*SH3BGRL2*
0.002935	-2.53814	0.257634	Q9UJU6	*DBNL*
0.031822	-1.11919	0.390214	Q9UQ80	*PA2G4*
0.003789	-2.23932	0.257634	Q9Y696	*CLIC4*

DEPs, differentially expressed proteins; BAV, bicuspid aortic valve.

https://dx.doi.org/10.21037/atm-21-3378